

Evaluation of Explicit-form Fundamental Solutions for Displacements and Stresses in 3D Anisotropic Elastic Solids

Y. C. Shiah¹, C. L. Tan² and V.G. Lee³

Abstract: The main impediment to the development of efficient algorithms for the stress analysis of 3D generally anisotropic elastic solids using the boundary element method (BEM) and the local boundary integral equation (LBIE) meshless method over the years is the complexity of the fundamental solutions and the computational burden to evaluate them. The ability to analytically simplify and reduce them into as explicit a form as possible so that they can be directly computed will offer significant cost savings. In addition, they facilitate easy implementation using existing numerical algorithms with the above-mentioned methods that have been developed for isotropy. In this paper, the explicit, real-variable forms of the fundamental solutions for the displacements and stresses are presented as algebraic expressions in terms of Stroh's eigenvalues. Although derived by one of the present authors some years ago, they have never been utilized in BEM or LBIE methods and their numerical evaluations have never been assessed. The veracity of these expressions and the direct manner with which numerical values can be obtained are demonstrated by some examples here.

Keyword: Fundamental solutions, Green's functions, anisotropic elasticity, Stroh's eigenvalues, boundary integral equations, boundary element method.

1 Introduction

In the formulation of the direct formulation of the boundary element method (BEM) and local boundary integral equation (LBIE) meshless methods, a key requirement is the availability of the fundamental solutions or Green's functions to the governing differential equations for the physical problem. For elastostatics, they correspond to the solutions for displacements and the stresses or tractions due to a unit point

¹ Dept. of Aerospace and Systems Engineering, Feng Chia University, Taichung, Taiwan, R.O.C.

² Dept. of Mechanical & Aerospace Engineering, Carleton University, Ottawa, Canada K1S 5B6

³ Dept. of Civil Engineering, National Chi Nan University, Nantou, Taiwan, R.O.C.

load in an infinite body. An efficient scheme to evaluate these Green's functions is important for the development of a robust and successful computational tool for the stress analysis of 3D elastic solids. In isotropic elasticity, they can be expressed in relatively simple, explicit forms; the computational effort for their evaluation has therefore not been a serious issue. This is also the case for 2D anisotropic elasticity [see, e.g., Shah *et al.* (2006), Shiah *et al.* (2006)]. Due to their mathematical complexity, the same cannot be said for 3D general anisotropy, however, and their numerical evaluation has remained a subject of research, particularly in the BEM community.

Green's functions have been developed for specific applications in anisotropic elasticity and non-homogeneous isotropy [see, e.g. Yang and Tewary (2006), Criado *et al.* (2007)]. For a 3D generally anisotropic elastic solid, the Green's function for the displacement field due to a unit point load has been derived by Lifschitz and Rozentsweig (1947). It was expressed as a line integral around a unit circle with the integrand containing the Christoffel matrix defined in terms of the elastic material constants. The evaluation of this integral and its derivatives into simpler analytical forms as well as the development of computationally efficient schemes for their numerical evaluation have been a focus of several investigators in the past several decades [see, e.g. Synge (1957), Barnett (1972), Wilson and Cruse (1978), Chen and Lin (1995), Ting and Lee (1997), Nakamura and Tanuma (1997), Wang (1997), Sales and Gray (1998), Pan and Yuan (2000), Tonon *et al.* (2001), Lee (2003), Phan *et al.* (2004), and Wang and Denda (2007)]. Wilson and Cruse (1978) were the first to implement a numerical formulation of the BEM for 3D stress analysis of a generally anisotropic solid using the solution of Lifschitz and Rozentsweig (1947). In their algorithm, a data- base for the evaluated point load solutions and their derivatives is generated, and interpolation of these values is performed in the BEM calculations. Sales and Gray (1998) improved significantly on the efficiency of the Wilson-Cruse approach by transforming the integrand of the line integral for the Green's function, using the calculus of residues, into a rational function. However, a concern of the Sales-Gray algorithm was its numerical instability when multiple poles of the residue are present. This was, however, overcome by an extension of the work by Phan *et al.* (2004). Employing the Radon transform and the calculus of residues, Wang (1997) derived an explicit algebraic expression for the displacement Green's function; no numerical results were presented, however. Instead, his work was implemented by Tonon *et al.* (2001) in a BEM formulation, and the numerical evaluation of the Green's function involves contour integration over a rectangular parallelepiped. It is assumed in these works that the roots of the sextic equation are distinct. Recently, Wang and Denda (2007) have also presented a BEM algorithm for 3D generally anisotropic elasticity in which the Green's function for

displacements is expressed in terms of a contour integral over a semi-circle. Analytical solution of the integral is obtained over triangular boundary elements with piecewise linear interpolation function in their BEM implementation.

An alternative, explicit solution of the displacement fundamental solution in a 3D anisotropic body based on Stroh's formalism has also been derived by one of the present authors in Ting and Lee (1997). It is simpler in form to that obtained by Wang (1997) and is expressed primarily in terms of Stroh's eigenvalues. It remains valid in the degenerate cases of equal eigenvalues. The explicit analytical expressions for the derivatives of Green's displacements for up to second order in terms of these eigenvalues were further developed in Lee (2003) by following the Fourier integral solutions developed by Barnett (1972), using the Cauchy residues theorem. Surprisingly, these expressions have never been utilized in any numerical method, such as the BEM or LBIE method, at least until very recently for the special case of transverse isotropy [Tavara *et al.* (2008)]. This may be because of no numerical evaluations are presented in the above-mentioned two papers, nor have the issues, if any, involved in doing so, ever been discussed. Perhaps for these reasons, these expressions have also mistakenly been perceived, as has been reported by some, as being too complex, and involve tedious calculations. The aim of this paper is to rectify the misperception.

The present authors have very recently demonstrated the relative ease of calculating the Green's function for displacements using the explicit solution [Shiah *et al.* (2008)]. However, the interpolation-finite difference scheme as proposed by Tonon *et al.* (2001) to calculate the derivatives of displacements, and thence the corresponding fundamental solution for the stresses, was employed in that study. In this article, the formulations presented in Lee (2003) are further implemented into a FORTRAN code to calculate the Green's function for stresses in a generally 3D anisotropic medium. For completeness, those for the displacement fundamental solutions [Ting and Lee (1997)] are also presented here. The veracity of these exact formulations and the direct manner in which these analytical solutions can be computed, are demonstrated by two examples for which independent exact solutions can be found. The interpolation-finite difference scheme mentioned above to obtain the approximate solution for the stresses is also employed for comparison of the numerical values obtained. It will be seen that the only numerical technique required in the computations of these explicit forms of the Green's functions is for the determination of the Stroh's eigenvalues.

2 Fundamental solution for displacements

The boundary integral equation (BIE), which relates the nodal displacements u_j and tractions t_j at the boundary S of the homogeneous elastic domain, is written in

indicial notation as

$$C_{ij}u_i(P) + \int_S u_i(Q)T_{ij}(P,Q)dS = \int_S t_i(Q)U_{ij}(P,Q)dS + \int_\Omega X_i(q)U_{ij}(P,q)d\Omega \quad (1)$$

where the leading coefficient $C_{ij}(P)$ depends upon the local geometry of S at the source point P ; $U_{ij}(P, Q) \equiv \mathbf{U}(\mathbf{x})$, and $T_{ij}^*(P, Q)$ represent the fundamental solutions of displacements and tractions, respectively, in the x_i -direction at the field point Q due to a unit load in the x_j -direction at P in a homogeneous infinite body. Computation of the fundamental solution of displacements, also often referred to as the Green's function, for generally anisotropic materials proposed in Ting and Lee (1997) was very recently discussed in Shiah *et al.* (2008). The main focus of this paper is to numerically evaluate the analytical spatial derivatives of this Green's function, $U_{ij,l}(P, Q)$, from which the corresponding solutions for the stresses and tractions are obtained. Nevertheless, for completeness, it is useful first to briefly review the derivation of this explicit closed-form solution of the Green's function for displacements.

Let a concentrated unit load \mathbf{f} be applied at the origin $\mathbf{x}=0$ in the three-dimensional space of a general anisotropic material. By taking Fourier transforms of the equilibrium equation, solving for the transformed displacements, and performing the inverse transforms, one may obtain the fundamental solution for displacements in the infinite space expressed as [Ting and Lee (1997)]

$$\mathbf{U} = \frac{1}{8\pi^3} \int_{-\infty}^{\infty} \int_{-\infty}^{\infty} \int_{-\infty}^{\infty} \mathbf{Z}^{-1}(\mathbf{k})e^{-i\mathbf{k}\cdot\mathbf{x}}dk_1dk_2dk_3 \quad (2)$$

where k_i ($i=1, 2, 3$) is the transformed parameter; \mathbf{Z}^{-1} is the inverse matrix of $\mathbf{Z} \equiv Z_{ik}(\mathbf{k}) = C_{ijks}k_jk_s$; and $C_{ijks} \equiv \mathbf{C}$ is the elastic stiffness tensor of the anisotropic material. The triple integration in eq. (2) can be transformed first into an integration over a unit sphere, and then be further reduced to a contour integral around the unit circle as [Barnett (1972), Synge (1957)]

$$U_{ij} = \frac{1}{8\pi^2r} \int_0^{2\pi} Z_{ij}^{-1}(k(\psi))d\psi, \quad (3)$$

where r is the radial distance between the source point at the origin and the field point at $\mathbf{x}=(x_1, x_2, x_3)$. In eq. (3), the integral is taken around the unit circle $|\mathbf{n}^*| = 1$ on the oblique plane normal to \mathbf{x} ; the unit vector \mathbf{n}^* on the oblique plane can be written in terms of an arbitrary parameter ψ as

$$\mathbf{n}^* = \mathbf{n} \cos \psi + \mathbf{m} \sin \psi, \quad (4)$$

where the vectors \mathbf{n} , \mathbf{m} along with \mathbf{x}/r form a right-handed triad $[\mathbf{n}, \mathbf{m}, \mathbf{x}/r]$. With reference to Figure 1, the general form of \mathbf{n} and \mathbf{m} can be expressed as

$$\begin{aligned} \mathbf{n} &= (\cos \phi \cos \theta, \cos \phi \sin \theta, -\sin \phi), \\ \mathbf{m} &= (-\sin \theta, \cos \theta, 0). \end{aligned} \tag{5}$$

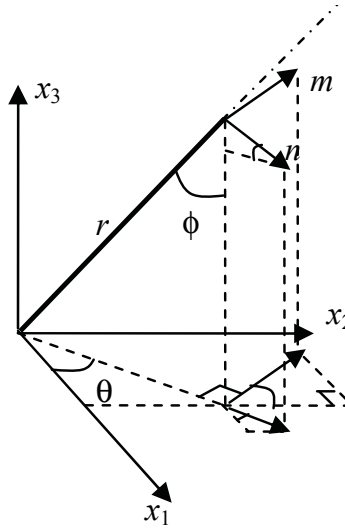


Figure 1: Definition of the unit vectors \mathbf{n} , \mathbf{m}

Equation (3) can thus be rewritten as

$$Z_{ik}(\psi) = C_{ijks}(n_j \cos \psi + m_j \sin \psi)(n_s \cos \psi + m_s \sin \psi). \tag{6}$$

By defining the following three tensors [Ting (1996)],

$$Q_{ik} = C_{ijks}n_jn_s, R_{ik} = C_{ijks}n_jm_s, T_{ik} = C_{ijks}m_jm_s, \tag{7}$$

eq. (6) can be rewritten into a simple form,

$$\mathbf{Z}(\psi) = \cos^2 \psi \mathbf{\Gamma}(p), \tag{8}$$

where $p = \tan \psi$, and $\mathbf{\Gamma}(p)$ is given by

$$\mathbf{\Gamma}(p) = \mathbf{Q} + p(\mathbf{R} + \mathbf{R}^T) + p^2\mathbf{T}. \tag{9}$$

By letting $\mathbf{V} = \mathbf{R} + \mathbf{R}^T$, eq. (9) may also be rewritten as

$$\mathbf{\Gamma}(p) = \mathbf{Q} + p\mathbf{V} + p^2\mathbf{T}. \tag{10}$$

Setting the determinant, $|\mathbf{\Gamma}(p)|$, to zero leads to a sextic equation in p which has six independent roots in general. By defining a matrix, $\mathbf{H}[\mathbf{x}]$, which depends only on the direction of \mathbf{x} and not its magnitude (hence the notation $[\mathbf{x}]$ instead of (\mathbf{x}) in the term), as

$$\mathbf{H}[\mathbf{x}] = \frac{1}{\pi} \int_{-\pi/2}^{\pi/2} \mathbf{Z}^{-1}(\psi) d\psi, \tag{11}$$

the Green's displacements can be expressed as

$$\mathbf{U}(\mathbf{x}) = \frac{1}{4\pi r} \mathbf{H}[\mathbf{x}]. \tag{12}$$

The limits of the integral in eq. (11) follows from the fact that $\mathbf{Z}(\psi)$ is periodic in ψ . The six roots of the sextic equation are the Stroh eigenvalues; they must be complex for the strain energy to be positive and they appear as three pairs of complex conjugates. It can be proved [Hagedorn (2000)] that the sextic equation is not analytically tractable. However, the computational effort to find these roots numerically is not, by any means, as demanding as compared with the numerical burden of performing the integration of eq. (11).

For an oblique plane, $\mathbf{H}[\mathbf{x}]$ remains symmetric and positive definite and so is the Green's function $\mathbf{U}(\mathbf{x})$. By writing the complex roots as

$$p_v = \alpha_v + i\beta_v, \quad \beta_v > 0, \quad (v = 1, 2, 3), \tag{13}$$

where both α_v and β_v are real, $\mathbf{H}[\mathbf{x}]$ can be expressed as [Ting and Lee (1997)]

$$\mathbf{H}[\mathbf{x}] = \frac{1}{|\mathbf{T}|} \sum_{t=1}^3 \frac{\hat{\mathbf{\Gamma}}(p_t)}{\beta_t (p_t - p_{t+1})(p_t - \bar{p}_{t+1})(p_t - p_{t+2})(p_t - \bar{p}_{t+2})}. \tag{14}$$

In eq. (14), the subscript t follows the cyclic rule $t = (t - 3)$ if $t > 3$, and $\hat{\mathbf{\Gamma}}$ is the adjoint of $\mathbf{\Gamma}$ which can be shown to be a polynomial in p of degree four. This equation provides an explicit expression of the Barnett-Lothe tensor $\mathbf{H}[\mathbf{x}]$, and hence the Green's function $\mathbf{U}(\mathbf{x})$, in terms of the Stroh eigenvalues p_v for general anisotropic elastic materials. It is evident that the expression for $\mathbf{H}[\mathbf{x}]$ above cannot be valid for the degenerate cases when there are repeated roots, i.e. when $p_t = p_{t+1}$ or

$p_t = p_{t+2}$. This problem may be resolved [Ting and Lee (1997)] by rewriting $\mathbf{H}[\mathbf{x}]$ as

$$\mathbf{H}[\mathbf{x}] = \frac{1}{|\mathbf{T}|} \sum_{n=0}^4 q_n \hat{\mathbf{\Gamma}}^{(n)}, \quad (15)$$

where q_n is given by

$$q_n = \begin{cases} \left\{ \frac{-1}{2\beta_1\beta_2\beta_3} \left[\text{Re} \left\{ \sum_{t=1}^3 \frac{p_t^n}{(p_t - \bar{p}_{t+1})(p_t - \bar{p}_{t+2})} \right\} - \delta_{n2} \right] \right\} & \text{for } n = 0, 1, 2, \\ \left\{ \frac{-1}{2\beta_1\beta_2\beta_3} \left[\text{Re} \left\{ \sum_{t=1}^3 \frac{p_t^{n-2} \bar{p}_{t+1} \bar{p}_{t+2}}{(p_t - \bar{p}_{t+1})(p_t - \bar{p}_{t+2})} \right\} \right] \right\} & \text{for } n = 3, 4, \end{cases} \quad (16)$$

In eq. (16), $\text{Re}\{\}$ represents the operation of taking real part, and δ_{mn} is the Kronecker delta. The components of $\hat{\mathbf{\Gamma}}^{(n)}$, namely, $\hat{\Gamma}_{ij}^{(n)}$, may then be expressed as

$$\hat{\Gamma}_{ij}^{(n)} = \tilde{\Gamma}_{(i+1)(j+1)(i+2)(j+2)}^{(n)} - \tilde{\Gamma}_{(i+1)(j+2)(i+2)(j+1)}^{(n)}, \quad (i, j = 1, 2, 3), \quad (17)$$

following some basic algebraic manipulations. Also, in eq. (16), the subscript t follows the cyclic rule as described before, and the 4-order tensor $\tilde{\mathbf{\Gamma}}^{(n)}$ is given by

$$\begin{aligned} \tilde{\Gamma}_{pqrs}^{(4)} &= T_{pq} T_{rs}, \\ \tilde{\Gamma}_{pqrs}^{(3)} &= V_{pq} T_{rs} + T_{pq} V_{rs}, \\ \tilde{\Gamma}_{pqrs}^{(2)} &= T_{pq} Q_{rs} + T_{rs} Q_{pq} + V_{pq} V_{rs}, \\ \tilde{\Gamma}_{pqrs}^{(1)} &= V_{pq} Q_{rs} + V_{rs} Q_{pq}, \\ \tilde{\Gamma}_{pqrs}^{(0)} &= Q_{pq} Q_{rs}. \end{aligned} \quad (18)$$

Once the Stroh's eigenvalues have been determined, the calculations in eqs. (15)-(18) are relatively straightforward, involving just standard matrix multiplications; they are easy to be programmed into a computer code.

3 Fundamental solution for stresses

The Green's function for displacements and its derivatives are essential for evaluating the elastic fields and energies associated with various inclusion and inhomogeneity problems of an anisotropic body. For use with numerical methods, such as in the direct BEM formulation of eq. (1), computation of the fundamental solution for tractions T_{ij}^* is also required. This may be carried out using

$$T_{ij}^* = (\sigma_{ik} N_k)_j, \quad (19)$$

where σ_{ik} is the fundamental solution for stresses at a field point due to a concentrated force applied in the x_j direction at the source point, and N_k are components of the outward normal vector on the surface at the former. To determine the stresses, denoted also by σ_j herein, the generalized Hooke's law is applied, as follows,

$$\sigma_j = C\epsilon_j, \tag{20}$$

where

$$\sigma_l = (\sigma_{11}, \sigma_{22}, \sigma_{33}, \sigma_{23}, \sigma_{13}, \sigma_{12})_l^T, \tag{21}$$

$$\epsilon_l = (\epsilon_{11}, \epsilon_{22}, \epsilon_{33}, 2\epsilon_{23}, 2\epsilon_{13}, 2\epsilon_{12})_l^T. \tag{22}$$

In eq. (22b), the strains $(\epsilon_{ik})_j$ are computed using

$$(\epsilon_{ij})_l = (U_{il,j} + U_{jl,i}) / 2. \tag{23}$$

From the foregoing, it is clear that the derivative of the fundamental solution for displacements, $U_{ij,l}$, must first be obtained in order to evaluate the fundamental solution for stresses or tractions. This will now be dealt with.

Instead of analytically differentiating U_{ij} , Tonon *et al.* (2001) suggested a relatively simple way to obtain $U_{ij,l}$ by a simple Lagrange interpolation scheme that results in a finite difference equation:

$$U_{ij,l}(\mathbf{x}) \cong \frac{U_{ij}(\mathbf{x} + \Delta_l) - U_{ij}(\mathbf{x} - \Delta_l)}{2h}, \quad (l = 1, 2, 3), \tag{24}$$

where Δ_l represents an increment in the abscissa direction of x_l due to an interval change of h ; they had used $h = r \times 10^{-6}$, in their study. In the present work, however, emphasis is on the analytical formulation derived by one of the present authors, Lee (2003); since it is analytically exact, the concern for the choice of step size does not arise. The key steps in the derivation of the expressions and the algorithm for computing the derivatives of the Green's function for displacement are presented below.

Using the spherical coordinate system, the unit position vector $\mathbf{y} = \frac{\mathbf{x}}{r}$ are given by

$$y_1 = \sin \varphi \cos \theta, \quad y_2 = \sin \varphi \sin \theta, \quad y_3 = \cos \varphi. \tag{25}$$

By performing differentiation on eq. (3) and using the same integration procedure as employed in reducing eq.(20) to eq (3), the first derivative of Green's function can be obtained as

$$U_{ij,l} = \frac{1}{4\pi^2 r^2} \int_0^\pi \left(-y_l \mathbf{Z}_{ij}^{-1} + k_l F_{ij} \right) d\psi, \tag{26}$$

where F_{ij} is given by

$$F_{ij} = C_{stnw} Z_{is}^{-1} Z_{nj}^{-1} (k_t y_w + k_w y_t), \quad (27)$$

Due to the complexity of the integrand in material anisotropy, the evaluation of eq. (26) presents extreme difficulty for practical applications, and have only been performed numerically for very limited cases in the past [Barnett (1972), Chen and Lin (2001)]. Closer examination of the integrand of this integral reveals that the result depends only on the forms of \mathbf{Z}^{-1} and \mathbf{k} , which are both functions of ψ . Also, since the component of \mathbf{n} is independent of ψ and will not affect the integration result, one may introduce an integral \mathbf{M} defined as follows:

$$M_{ijklmn} = \int_0^\pi k_i k_j Z_{kl}^{-1} Z_{mn}^{-1} d\psi. \quad (28)$$

Due to the symmetry of \mathbf{Z} and \mathbf{Z}^{-1} , each sub-index of \mathbf{Z}^{-1} appearing in \mathbf{M} is interchangeable. As a consequence, the sub-indices i and j shown in \mathbf{M} are interchangeable too. According to the integral definition given by eq. (26), the derivative of the Green's function for displacements can thus be expressed as

$$U_{ij,l} = \frac{1}{4\pi^2 r^2} [-\pi y_l H_{ij} + C_{pqrs} (y_s M_{lqiprj} + y_q M_{sliprj})] \quad (29)$$

In the integral \mathbf{M} of eq. (28), the terms k_i and Z_{kl}^{-1} are homogeneous and are of degree $+1$ and -2 in $\cos \psi$, respectively. With the use of eq. (8) and the change of variables as $\cos^2 \psi dp = d\psi$, the integral in eq. (28) becomes

$$M_{ijklmn} = \int_{-\infty}^{\infty} \frac{\Phi_{ijklmn}(p)}{(p-p_1)^2 (p-p_2)^2 (p-p_3)^2} dp, \quad (30)$$

where the function $\Phi_{ijklmn}(p)$ can be shown to be [Lee(2003)]

$$\Phi_{ijklmn}(p) = \frac{B_{ij}(p) \hat{\Gamma}_{kl}(p) \hat{\Gamma}_{mn}(p)}{(p-\bar{p}_1)^2 (p-\bar{p}_2)^2 (p-\bar{p}_3)^2}, \quad (31)$$

and $B_{ij}(p)$ is given by

$$B_{ij}(p) = n_i n_j + (n_i m_j + m_i n_j) p + m_i m_j p^2. \quad (32)$$

Using the Cauchy's residue theorem, the explicit expression of M_{ijklmn} is given in terms of the Stroh's eigenvalue p_t as

$$M_{ijklmn} = \frac{2\pi i}{|\mathbf{T}|^2} \sum_{t=1}^3 \frac{\left[\Phi'_{ijklmn}(p_t) - 2\Phi_{ijklmn}(p_t) \times \left(\frac{1}{p_t - p_{t+1}} + \frac{1}{p_t - p_{t+2}} \right) \right]}{(p_t - p_{t+1})^2 (p_t - p_{t+2})^2}, \quad (33)$$

in which the prime denotes differentiation of Φ with respect to the argument p ; p_{t+1} and p_{t+2} follow the cyclic rule for $t > 2$ as mentioned earlier. It is unnecessary to rewrite the term $\Phi'_{ijklmn}(p_t)$ in eq. (33) as a fully explicit expression, since it is a relatively simple matter to program the functions $B(p)$, $\hat{\Gamma}(p)$, $(p - \bar{p}_t)^2$ and their derivatives into subroutines in the computer code and then apply the chain rule in the differentiation.

It should be noted that although eq. (33) appears to be in a complex form, its imaginary part will eventually disappear to yield real variables. Also it should be mentioned that this expression is ill-defined when repeated roots of the sextic equation occurs (i.e. $p_t = p_{t+1}$ or $p_t = p_{t+1} = p_{t+2}$). However, this situation is not commonly encountered and a simple way to overcome this problem if it occurs is to introduce a small perturbation to one of the repeated roots when computing eq. (33). Work is currently in progress to seek an analytical remedy to this issue.

4 Numerical examples

In this section, some example results of the numerical evaluation of the above exact expressions for the 3D fundamental solutions of displacements and stresses in a generally anisotropic solid are presented. Except for some care that may be exercised to determine the Stroh's eigenvalues on the oblique plane normal to the radial vector between the source and field points, the steps and calculations involved to obtain the displacement and stress components are relatively straightforward indeed. In the present work, Laguerre's method (see, e.g. Press *et al.* (1990)) is employed to solve the sextic equations for the eigenvalues. As has been discussed earlier, explicit, exact, analytical solutions for the displacement and stress Green's functions for a generally anisotropic body are very scarce indeed in the literature. The veracity of the present formulations can, however, still be established using those for transverse isotropy where several closed-form expressions exist; they have been derived using various approaches [see, e.g., Willis (1965), Elliot (1948), Chen (1966), Pan and Chou (1976), and Loloi (2000)]. In the present study, the exact solutions of Pan and Chou (1976) are used for comparison. To this end, numerical solutions for the displacements and stresses at an arbitrary field point are first obtained for this degenerate case of transverse isotropy using a set of material constants. To check the case for general anisotropy, it is also possible to still use the same transversely isotropic material, as follows. By rotating the material axes successively about the x_2 -axis and x_3 -axis, a fully populated stiffness matrix \mathbf{C} will be obtained which has all the features of general anisotropy. The exact solutions for this set of properties can be determined by carrying out the corresponding coordinate transformations of the closed-form solutions for transverse isotropy. This allows comparison of the results using the above general anisotropic formulations.

Consider, as Example 1, a transversely isotropic, linearly elastic solid with its isotropic plane parallel to the $x_1 - x_2$ plane and having the following material constants for its stiffness matrix \mathbf{C} :

$$\mathbf{C} = \begin{bmatrix} 120 & 90 & 70 & 0 & 0 & 0 \\ 90 & 120 & 70 & 0 & 0 & 0 \\ 70 & 70 & 50 & 0 & 0 & 0 \\ 0 & 0 & 0 & 30 & 0 & 0 \\ 0 & 0 & 0 & 0 & 30 & 0 \\ 0 & 0 & 0 & 0 & 0 & 15 \end{bmatrix} \times 10^7 \text{N/m}^2. \quad (34)$$

At the source point which is located at the origin of the coordinate system, a unit load (1 N) is applied. The displacements and stresses at a field point located at $\mathbf{x} = (-1.2, 0.6, 1)$ (m) are to be determined. The choice of this field point is arbitrary and is purely for the purpose of demonstration here. The computed Green's function solution for the displacements using the above formulation of Ting and Lee (1997) at this field point are listed in Table 1 together with the corresponding values obtained using the closed-form solution of Pan and Chou (1976). As can be seen, the percentage deviation between the two sets of exact solutions is typically of the order of 10^{-7} .

As explained in the previous section, two possible means of computing the Green's function for stresses may be employed. One is based on Lagrange interpolation which leads to a finite difference scheme of the displacement fundamental solution to obtain its derivatives for the strains, and from which the constitutive relations are invoked to obtain the stresses. The second is the exact formulation presented above using the explicit real-variable explicit expressions based on Lee's (2003) solution for the derivatives of Green's function for displacement. The computed values of the Green's function for the stresses at this field point using both these approaches are shown in Table 2. For the results using the former approach, an interval $h = (r \times 10^{-6})$ is employed; the choice of this value will be further discussed later below. Also shown are the closed-form solutions of Pan and Chou (1976). As can be seen, the agreement of the numerical results is excellent indeed. The percentage deviations of those values calculated directly from the exact formulations are in the order of 10^{-9} to 10^{-7} ; the corresponding percentage deviations of the results based on the finite difference scheme, although still very small, are typically two to three orders larger.

Next, in Example 2, consider the same material constants as in the first example but with rotations of the material axes. By successive rotations of the x_2 -axis and x_3 -axis by 45° and 150° counter-clockwise, respectively, the following elastic stiffness

Table 1: Comparison of the Green’s function solution for displacements- Example 1

(i, j)	$U_{ij} \times 10^{-10}(\text{m})$ [present;Ting and Lee (1997)]	$U_{ij} \times 10^{-10}(\text{m})$ [Pan & Chou (1976)]	$ Error\% $
(1,1)	2.9458898019269	2.945889814144619	4.15E-07
(1,2)	-0.6620028549991	-0.662002856228628	1.86E-07
(1,3)	-1.9820333647348	-1.982033378913727	7.15E-07
(2,2)	1.9528855224043	1.952885529805554	3.79E-07
(2,3)	0.9910166884868	0.991016689456864	9.79E-08
(3,3)	4.6467329250087	4.646732946994783	4.73E-07

matrix which has the features of general anisotropy may be obtained:

$$\mathbf{C} = \begin{bmatrix} 114.84 & 75.78 & 55.62 & -13.43 & -10.28 & -5.14 \\ 75.78 & 121.09 & 71.87 & -0.31 & -13.53 & -0.27 \\ 55.62 & 71.87 & 107.49 & -8.75 & -15.15 & -14.07 \\ -13.43 & -0.31 & -8.75 & 18.75 & -6.49 & 1.62 \\ -10.28 & -13.53 & -15.15 & -6.49 & 11.25 & -4.68 \\ -5.14 & -0.27 & -14.07 & 1.62 & -4.68 & 18.28 \end{bmatrix} \times 10^7(\text{N/m}^2). \tag{35}$$

In the rotated coordinate system, the field point has new coordinates (1.6472193, 0.258202, -0.1414213). The analytical solution for this case can now be obtained by coordinate transformation of the closed-form solution of Pan and Chou (1976). The Green’s displacements and stresses computed by the present algorithms and the closed-form solutions are listed in Table 3 and Table 4, respectively. From these tables, it can be seen that the numerical solutions obtained by the present algorithms which directly computed the exact explicit formulations, are indeed in excellent agreement with the closed-form solutions of Pan and Chou (1976), the percentage deviations being typically of the order of 10^{-6} . For those solutions of the stresses obtained using the finite difference scheme, the percentage deviations, are typically a few orders of magnitude larger; the significance of this percentage error will now be discussed.

The percentage error in the numerical results for the stresses using the finite difference scheme depends on the interval size h . It is therefore worth investigating the effects of varying this interval size. Figures 2-4 show the percentage errors of the stress components obtained using this scheme when h is varied from $(r \times 10^{-3})$ to $(r \times 10^{-6})$ for the two examples above; it can be seen that the errors clearly

Table 2: Comparison of the Green’s function solution for stresses $\sigma_l \times 10^{-2}$ (N/m²)-
Example 1

(i, j)		Pan and Chou (1976)	Finite difference scheme		Error%
			A	Present; Lee (2003)	
$(l=1)$	(1,1)	7.7611796589675	A	7.7611812101652	1.99E-05
			B	7.7611796843199	3.26E-07
	(1,2)	-2.7321608867554	A	-2.7321607493153	5.03E-06
			B	-2.7321608687902	6.57E-07
	(1,3)	-5.9568612502977	A	-5.9568610938445	2.62E-06
			B	-5.9568612074077	7.20E-07
	(2,2)	5.3806830859151	A	5.3806855438633	4.56E-05
			B	5.3806830837096	4.09E-08
	(2,3)	3.4443631969267	A	3.4443623004460	2.60E-05
			B	3.4443631851774	3.41E-07
	(3,3)	4.8302346086816	A	4.8302361640289	3.22E-05
			B	4.8302346100601	2.85E-08
$(l=2)$	(1,1)	-5.2547856369595	A	-5.2547798735480	1.09E-06
			B	-5.2547856287880	1.55E-09
	(1,2)	0.3354335881748	A	0.3354334327371	4.63E-07
			B	0.3354335867710	4.18E-09
	(1,3)	3.4443631969936	A	3.4443645953013	4.05E-07
			B	3.4443631773097	5.71E-09
	(2,2)	-1.3161457366876	A	-1.3161396455678	4.62E-06
			B	-1.3161457448772	6.22E-09
	(2,3)	-0.7903164557164	A	-0.7903178618048	1.77E-06
			B	-0.7903164567530	1.31E-09
	(3,3)	-2.4151173046279	A	-2.4151130794400	1.74E-06
			B	-2.4151173081502	1.45E-09
$(l=3)$	(1,1)	-10.0932019147208	A	-10.093203557786	1.62E-05
			B	-10.093201932100	1.72E-07
	(1,2)	2.6152256766399	A	2.6152261501253	1.81E-05
			B	2.6152256474065	1.11E-06
	(1,3)	7.6445199610860	A	7.6445205876963	8.19E-06
			B	7.6445199101068	6.66E-07
	(2,2)	-6.1703633997610	A	-6.1703672410638	6.22E-05
			B	-6.1703634028720	5.04E-08
	(2,3)	-3.8222599805430	A	-3.8222568519541	8.18E-05
			B	-3.8222599699090	2.78E-07
	(3,3)	-6.3704333009050	A	-6.3704353431351	3.20E-05
			B	-6.3704333023360	2.24E-08

decrease to very small values when $h = (r \times 10^{-6})$. This is consistent with the investigation carried out by Tonon et al.(2001) mentioned earlier who had suggested $h = (r \times 10^{-6})$ be used. Notwithstanding the simplicity of this approach, the uncertainty of the errors introduced for a given interval size *may* remain an issue for some physical problems, such as when the distance r between the source and field points becomes relatively small. Thus, the exact real-variable expressions for the stress fundamental solution presented above should be preferred in LBIE and BEM formulations, not least because they are analytically exact. Interestingly, checks on the computational effort in their numerical evaluation for the two problems above show execution times which are quite similar to the finite difference scheme. This can be attributed to the fact that calculations involving much higher order tensors are involved using the exact analytical expressions, even though the Lagrange interpolation-finite difference scheme requires the computation of the displacement tensor at six points in the neighbourhood of the field point.

Finally, the use of the perturbation method to obtain the numerical values of the fundamental solution for the stresses in the degenerate case of repeated roots, eq. (13), of the sextic equation is demonstrated here.

Table 3: Comparison of the Green’s function solution for displacements- Example 2

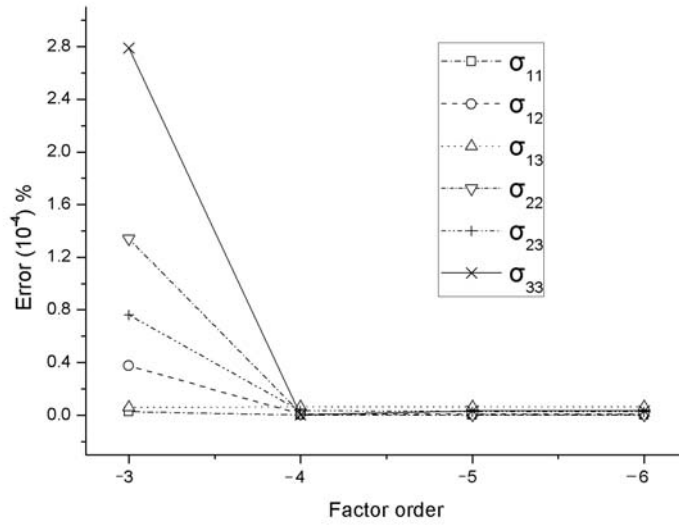
(i, j)	$U_{ij} \times 10^{-10}(\text{m})$ [Present; Ting and Lee (1997)]	$U_{ij} \times 10^{-10}(\text{m})$ [Pan and Chou (1976)]	Error%
(1,1)	5.8342437246382	5.8342435575081	2.86E-06
(1,2)	1.0720418072674	1.0720417719273	3.30E-06
(1,3)	0.8528106727866	0.8528106367402	4.23E-06
(2,2)	1.8969867699750	1.8969867317808	2.01E-06
(2,3)	0.2237317760902	0.2237317807810	2.10E-06
(3,3)	1.8142780193840	1.8142780016556	9.77E-07

For practical problems, it is usually not possible to pre-determine when the degeneracy occurs, as it depends on the position of the field point and the material properties. For the purpose of demonstration here, the field point is arbitrarily chosen to be (-0.1, 0.8, 1.5) and the roots are taken to be $p_1 = p_2 = p_3 = 1.0i$. The corresponding material properties which would give rise to these repeated roots were obtained in an inverse manner as

Table 4: Comparison of the Green’s function solution for stresses $\sigma_l \times 10^{-2}$ (N/m²)-
Example 2

(i, j)		Pan and Chou (1976)	A	Finite difference scheme	Error%
			B	Present; Lee (2003)	
$(l=1)$	(1,1)	-22.6566146252610	A	-22.6566218728510	3.19E-05
			B	-22.6566151547170	2.33E-06
	(1,2)	-2.7569131706591	A	-2.7569149714364	6.53E-05
			B	-2.7569133235326	5.54E-06
	(1,3)	1.8831988920288	A	1.8832019742508	1.63E-04
			B	1.8831988659465	1.38E-06
	(2,2)	-5.9400247001547	A	-5.9400331105838	1.41E-04
			B	-5.9400246520744	8.09E-07
	(2,3)	2.2325888473228	A	2.2325901584591	5.87E-05
			B	2.2325889664050	5.33E-06
	(3,3)	-0.7624389063255	A	-0.7624469411729	1.05E-03
			B	-0.7624385273813	4.97E-05
$(l=2)$	(1,1)	-5.6007670907344	A	-5.6007704514293	6.00E-05
			B	-5.6007672545850	2.92E-06
	(1,2)	0.9302943734292	A	0.9302917325645	2.83E-04
			B	0.9302943411858	3.46E-06
	(1,3)	-0.1468636258801	A	-0.1468629347811	4.70E-04
			B	-0.1468636116680	9.67E-06
	(2,2)	-0.9843275650484	A	-0.9843319656283	4.47E-04
			B	-0.9843275921341	2.75E-06
	(2,3)	0.1475933736669	A	0.1475949712153	1.08E-03
			B	0.1475933740711	2.73E-07
	(3,3)	0.0108181822340	A	0.0108186958769	4.74E-03
			B	0.0108182792238	8.96E-04
$(l=3)$	(1,1)	-2.1743905752618	A	-2.1743940943342	1.61E-04
			B	-2.1743906697108	4.34E-06
	(1,2)	-0.8025185590599	A	-0.8025183553638	2.53E-05
			B	-0.8025185982651	4.88E-06
	(1,3)	0.1187374636871	A	0.1187370785341	3.24E-04
			B	0.1187374941262	2.56E-05
	(2,2)	-0.9463894936384	A	-0.9463929723737	3.67E-04
			B	-0.9463894574277	3.82E-06
	(2,3)	0.3542444914073	A	0.3542458308903	3.78E-04
			B	0.3542444971618	1.62E-06
	(3,3)	-0.1756819265565	A	-0.1756829781131	5.98E-04
			B	-0.1756818880558	2.19E-05

(a) Example 1:



(b) Example 2:

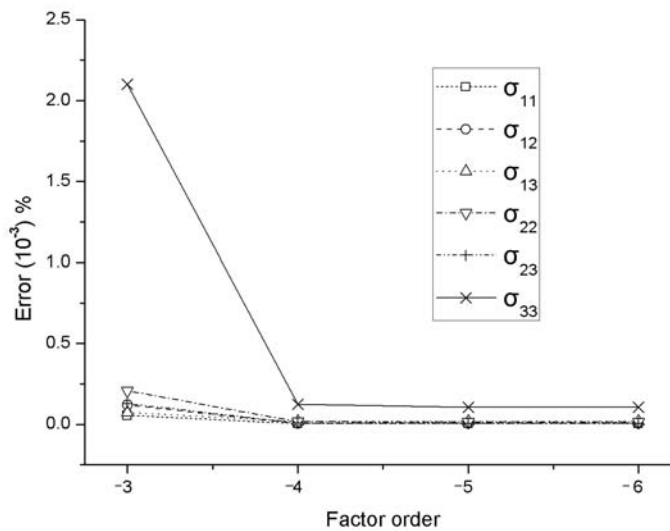
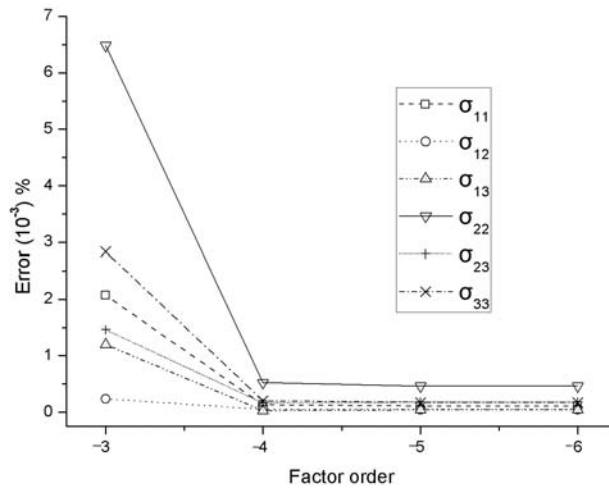


Figure 2: The percentage error of the stress calculations using the finite difference scheme for unit load applied in the x_1 -direction.

(a) Example 1:



(b) Example 2:

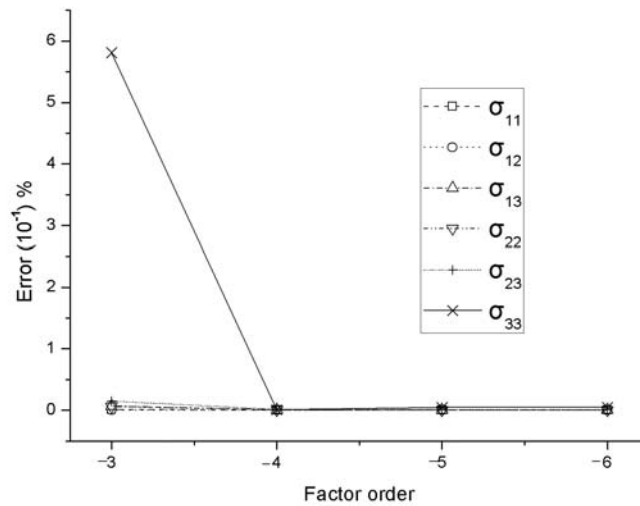
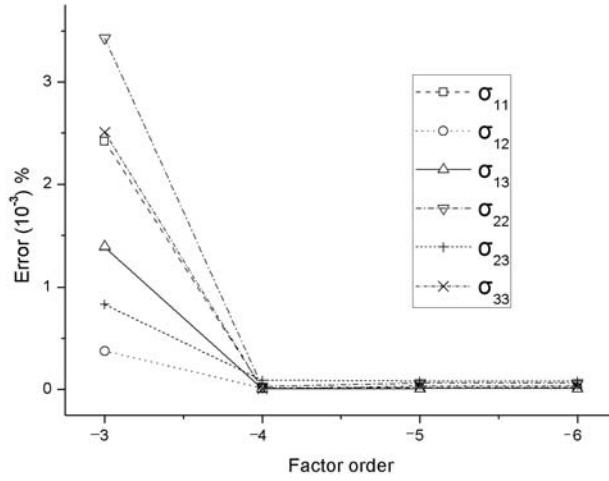


Figure 3: The percentage error of the stress calculations using the finite difference scheme for unit load applied in the x_2 -direction.

(a) Example 1:



(b) Example 2:

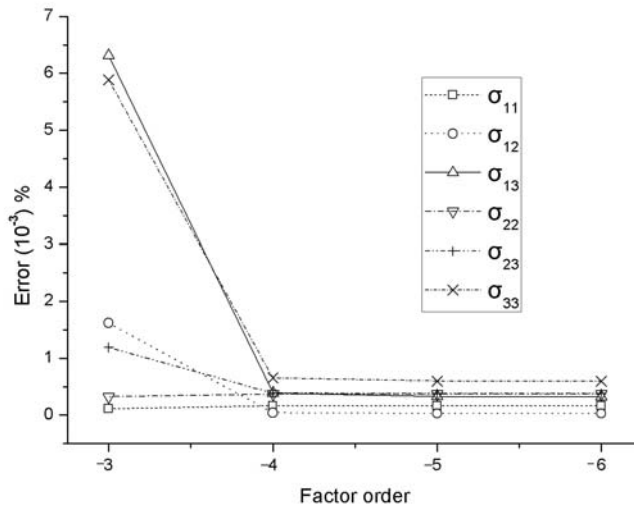


Figure 4: The percentage error of the stress calculations using the finite difference scheme for unit load applied in the x_3 -direction.

$$\mathbf{C} = \begin{pmatrix} 23.9953 & 23.5869 & 23.5894 & 0 & 0 & 0 \\ 23.5869 & 23.9953 & 23.5894 & 0 & 0 & 0 \\ 23.5894 & 23.5894 & 24 & 0 & 0 & 0 \\ 0 & 0 & 0 & 0.204124 & 0 & 0 \\ 0 & 0 & 0 & 0 & 0.204124 & 0 \\ 0 & 0 & 0 & 0 & 0 & 0.204165 \end{pmatrix} \text{ GPa}$$

The perturbation is automatically set by the Laguerre algorithm employed in the present work [Press *et al.* (1990)], and the roots for this set of material properties at the field point are numerically found to be

$$p_1 = (-0.5317745E - 02 + 0.1003090E + 01i)$$

$$p_2 = (0.0000000E + 00 + 0.9938080E + 00i)$$

$$p_3 = (0.5317599E - 02 + 0.1003101E + 01i)$$

Table 5 lists the computed results for the stress components when the unit load is applied in the x_1 -direction at the load point ($l = 1$) using the present Green’s function as well as the finite difference approach. The results are compared with those obtained from Pan and Chou’s (1976) analytical solution again. It can be seen that the percentage deviations of the Green’s function solutions with the perturbation, when compared with Pan and Chou’s (1976) solution, remain relatively small, although they are now of the same order of magnitude as those obtained using the finite difference approach of the displacement fundamental solution. Similar findings were obtained when the unit load at the source point is applied in the other two directions, i.e. when $l = 2$ and 3, and hence they are not shown here.

5 Conclusions

In this paper, explicit, real-variable, closed-form algebraic expressions for the fundamental solutions (or Green’s functions) for the displacements and stresses in a 3D generally anisotropic solid have been presented. Only the Stroh’s eigenvalues need to be numerically obtained in their evaluation; the formulations to determine the numerical values for the displacement and stress components are relatively straightforward indeed. Two examples, one involving transverse isotropic material properties and another having features of general anisotropy, have been presented to demonstrate the veracity of the formulations. An alternative procedure employing a Lagrange interpolation-finite difference scheme, used in other formulations previously, was also employed to check the numerical values of the Green’s function for the stresses obtained with the present exact formulation. Although the Green’s

Table 5: Comparison of the Green’s function solution for stresses σ_l (N/m²) - Example 3

(i, j)		Pan and Chou (1976)	A	Finite difference scheme	$ Error\% $
			B	Present; Lee (2003)	
$(l=1)$	(1,1)	0.80199483368655	A	0.8020735905499	9.82E-04
			B	0.8019178301599	9.60E-04
	(1,2)	-0.64150690788477	A	-0.6415058306542	1.68E-05
			B	-0.6415059961551	1.42E-05
	(1,3)	-1.20287734683087	A	-1.2028783129801	8.03E-05
			B	-1.2028789009552	1.29E-05
	(2,2)	0.49902858493179	A	0.4991050636860	1.53E-03
			B	0.4989507014977	1.56E-03
	(2,3)	0.95166560312409	A	0.9516663639051	7.99E-05
			B	0.9516663080837	7.41E-05
	(3,3)	1.77581631892687	A	1.7758944194638	4.32E-04
			B	1.7757408412432	4.25E-04

function for the stresses is ill-defined for repeated Stroh’s eigenvalues, the problem can be circumvented by a perturbation method. This has also been demonstrated in the paper. The explicitness of these exact fundamental solutions makes it suitable for relatively easy implementation into, e.g., existing BEM computer codes for 3D elastostatics. This has been achieved by the present authors, a full report of which will appear in a forthcoming paper when it has been fully tested.

References

Barnett, D.M. (1972): The precise evaluation of derivatives of the anisotropic elastic Green’s functions. *Phys. Stat. Sol.* (b) 49, 741-748.

Chen, T.; Lin, F.Z. (2001): Numerical evaluation of derivatives of the anisotropic elastic Green’s functions. *Mech. Res. Comm.*, 20, 501-506.

Chen, W.T. (1966): On some problems in transversely isotropic materials. *J. Appl. Mech.*, 33, 347-355.

Criado, R; Ortiz, J.E., Mantic, V; Gray, L.J.; Paris, F. (2007): Boundary element analysis of three-dimensional exponentially graded isotropic elastic solids, *CMES: Computer Modeling in Engineering & Sciences*, 22, 151-164.

Elliot, H.A. (1948): Three dimensional stress distributions in hexagonal aelotropic crystals. *Proc. Cambridge Phil. Soc.*, 44, 522-533.

Hagedorn, T.R. (2000): General formulas for solving solvable sextic equations. *J. Algebra*, 233, 704-757.

Lee, V.G. (2003): Explicit expression of derivatives of elastic Green's functions for general anisotropic materials. *Mech. Res. Comm.*, 30, 241-249.

Lifshitz I.M.; Rozenzweig, L.N. (1947): Construction of the Green tensor for the fundamental equation of elasticity theory in the case of unbounded elastically anisotropic medium, *Zh. Eksp. Teor. Fiz.*, 17, 783-791.

Loloi, M. (2000): Boundary integral equation solution of three dimensional elastostatic problems in transversely isotropic solids using closed-form fundamental solutions. *Int. J. Numer. Methods Engng.*, 48, 823-842.

Nakamura, G.; Tanuma, K. (1997): A formula for the fundamental solution of anisotropic elasticity. *Q. J. Mech. Appl. Math.*, 50, 179-194.

Pan, Y.C.; Chou, T.W. (1976): Point force solution for an infinite transversely isotropic solid. *J. Appl. Mech.*, 29, 225-236.

Pan, E.; Yuan, F.G. (2000): Boundary element analysis of three dimensional cracks in anisotropic solids. *Int. J. Numer. Methods Engng.*, 48, 211-237.

Phan, P.V.; Gray, L.J.; Kaplan, T. (2004): On the residue calculus evaluation of the 3D anisotropic elastic Green's function. *Comm. Numer. Methods Engng.*, 20, 335-341.

Press, W.H.; Flannery, B.P.; Teukolsky, S.A. (1990): *Numerical recipes (FORTRAN version)*, Cambridge University Press, Cambridge (U.K.).

Sales, M.A.; Gray, L.J. (1998): Evaluation of the anisotropic Green's function and its derivatives. *Comp. & Struct.*, 69, 247-254.

Shah, P.D.; Tan, C.L.; Wang, X. (2006): Evaluation of T-stress for an interface crack between dissimilar anisotropic materials using the boundary element method, *CMES: Computer Modeling in Engineering & Sciences*, 3, 185-198.

Shiah, P.D.; Lin, Y.C.; Tan, C.L. (2006): Boundary element analysis of thin, layered anisotropic bodies, *CMES: Computer Modeling in Engineering & Sciences*, 16, 15-26.

Shiah, Y.C.; Tan, C.L.; Lee, V.G.; Chen, Y.H. (2008): Evaluation of Green's functions for 3D anisotropic elastic solids. *Advances in Boundary Element Techniques IX, Proc. BeTeq 2008 Conf., Seville*, R. Abascal & M.H. Aliabadi (eds.), E.C. Ltd. (U.K.), 119-124.

Syngé, J.L. (1957): *The Hypercircle in Mathematical Physics*, Cambridge University Press, Cambridge.

Tavara, L.; Ortiz, J.E.; Mantic, V.; Paris, R. (2008): Unique real-variable expres-

sions of displacement and traction fundamental solutions covering all transversely isotropic materials for 3D BEM. *Int. J. Numer. Methods Engng.*, 74, 776-798.

Ting, T.C.T. (1996): *Anisotropic Elasticity*, Oxford University Press, Oxford (U.K.).

Ting, T.C.T.; Lee, V.G. (1997): The three-dimensional elastostic Green's function for general anisotropic linear elastic solid. *Q. J. Mech. Appl. Math.*, 50, 407-426.

Tonon, F.; Pan, E.; Amadei, B. (2001): Green's functions and boundary element method formulation for 3D anisotropic media. *Comp. & Struct.*, 79, 469-482.

Wang, C.Y. (1997): Elastic fields produced by a point source in solids of general anisotropy. *J. Engng. Math.*, 32, 41-52.

Wang, C.Y.; Denda, M. (2007): 3D BEM for general anisotropic elasticity. *Int. J. Solids Struct.*, 44, 7073-7091.

Willis, J.R. (1965): The elastic interaction energy of dislocation loops in anisotropic media. *Q. J. Mech. Appl. Math.*, 18, 419-433.

Wilson, R.B.; Cruse, T.A. (1978): Efficient implementation of anisotropic three dimensional boundary integral equation stress analysis. *Int. J. Numer. Methods Engng.*, 12, 1383-1397.

Yang, B.; Tewary, V.K. (2006): Efficient Green's function modeling of line and surface defects in multilayered anisotropic elastic and piezoelectric materials, *CMES: Computer Modeling in Engineering & Sciences.*, 15, 165-177.